Article

TRANSPARENT PROCESS

THE EMBO JOURNAL

Acidic cell elongation drives cell differentiation in the *Arabidopsis* root

Elena Pacifici[1], Riccardo Di Mambro[2], Raffaele Dello Ioio[1], Paolo Costantino[1,3] & Sabrina Sabatini[1,*]

Abstract

In multicellular systems, the control of cell size is fundamental in regulating the development and growth of the different organs and of the whole organism. In most systems, major changes in cell size can be observed during differentiation processes where cells change their volume to adapt their shape to their final function. How relevant changes in cell volume are in driving the differentiation program is a long-standing fundamental question in developmental biology. In the *Arabidopsis* root meristem, characteristic changes in the size of the distal meristematic cells identify cells that initiated the differentiation program. Here, we show that changes in cell size are essential for the initial steps of cell differentiation and that these changes depend on the concomitant activation by the plant hormone cytokinin of the EXPAs proteins and the AHA1 and AHA2 proton pumps. These findings identify a growth module that builds on a synergy between cytokinin-dependent pH modification and wall remodeling to drive differentiation through the mechanical control of cell walls.

Keywords cell differentiation; cell wall acidification; cell wall expansion; cytokinin; root meristem

Subject Categories Development & Differentiation; Plant Biology; Signal Transduction

DOI 10.15252/embj.201899134 | Received 1 February 2018 | Revised 12 June 2018 | Accepted 13 June 2018 | Published online 16 July 2018

The EMBO Journal (2018) 37: e99134

Introduction

Cell differentiation is a complex process through which cells acquire distinct identities and specialized functions. In most systems, initiation of cell differentiation is accompanied by characteristic post-mitotic changes in volume necessary for the cell to reach its final size and to adapt its shape to its function (Marshall *et al*, 2012). The significance of these changes in size and whether they can affect cell differentiation is still unclear. We used the *Arabidopsis* root, where the development of each tissue can be easily followed in time and space, to provide an answer to this long-standing fundamental question. In this system, each tissue arises from a single stem cell (Benfey & Scheres, 2000). Stem cells self-renew and produce daughter cells which undergo subsequent cycles of cell division, generating the meristematic zone (Benfey & Scheres, 2000). Characteristic changes in the size of the distal meristematic cells identify the position of the transition zone (TZ) a developmental boundary where cells lose their capacity to divide and start to differentiate (Fig 1A).

The positioning and maintenance of the TZ are important events during root organogenesis, as they ultimately determine the size of the root (Pacifici *et al*, 2015; Di Mambro *et al*, 2017). We have previously shown that the position of the TZ depends on the antagonistic activities of two plant hormones: cytokinin and auxin (Dello Ioio *et al*, 2008b; Di Mambro *et al*, 2017). Cytokinin activates the transcription factor *ARABIDOPSIS* RESPONSE REGULATOR 1 (ARR1), which in turn activates the *SHORT HYPOCOTYL 2* (*SHY2*) and the *GRETCHEN HAGEN 3.17* (*GH3.17*) genes involved in controlling, respectively, polar auxin transport and degradation (Dello Ioio *et al*, 2008b; Di Mambro *et al*, 2017). In this way, cytokinin shapes the graded distribution of auxin, positioning an auxin minimum in the topmost root meristematic cells, which acts as a positional signal that triggers cell differentiation (Di Mambro *et al*, 2017). Upon sensing this auxin minimum, cells start to differentiate, expanding in one direction (elongate) increasing their size (Di Mambro *et al*, 2017). Here, we set to understand the significance of these changes in size and whether they can affect the cell differentiation program.

In plants, cell expansion necessitates loosening of the cell wall structure (Cosgrove, 2005), a process mediated by proteins named α-expansins (EXPAs) that are located in the cell wall and activated by low apoplastic pH (Cosgrove, 2005). EXPAs disrupt non-covalent bonds between cell wall components thus allowing turgor-driven cell expansion (Cosgrove, 2005), but their role in plant organ development is only poorly understood (Cho & Cosgrove, 2000).

We set to demonstrate whether cell wall extensibility induced by *EXPA* genes is necessary for root cell elongation at the root TZ and, most importantly, whether this EXPA-controlled elongation affects cell differentiation thus controlling the position of the TZ and, consequently, root and root meristem size.

1 Dipartimento di Biologia e Biotecnologie, Laboratory of Functional Genomics and Proteomics of Model Systems, Università di Roma La Sapienza, Rome, Italy
2 Dipartimento di Biologia, Università di Pisa, Pisa, Italy
3 Istituto di Biologia e Medicina Molecolari, CNR, Rome, Italy
*Corresponding author. Tel: +39 06 49917916; Fax: +39 06 49917594; E-mail: sabrina.sabatini@uniroma1.it

It was previously reported that four members of the α-expansin subfamily, *EXPA1*, *EXPA10*, *EXPA14,* and *EXPA15,* are induced by cytokinin in the root (Bhargava *et al*, 2013). Since in the root cytokinin is involved in controlling cell differentiation initiation (Pacifici *et al*, 2015), we focused on these four genes. We first analyzed the root meristem phenotype of the loss-of-function mutants *expa1, expa10*, *expa14,* and *expa15*. Interestingly, while the *expa1* mutant displays a larger meristem and a longer root than the wild type (WT), no root phenotype could be detected in the *expa10*, *expa14,* and *expa15* single mutants (Figs 1A–E and EV1B). However, enlarged meristems and longer roots could be observed in the double mutants, *expa15;expa10, expa14;expa10,* and *expa14;expa15*, suggesting that, except for EXPA1, these expansins act redundantly (Fig EV1A–C and D). To confirm that the change in root meristem size observed in the *expa1* mutant is the result of a change in TZ position, we analyzed the *CYCB1;1:GUS* cell cycle reporter (highlighting meristematic zone) and the RCH2 marker line (highlighting cell at the elongation/differentiation zone; Dello Ioio *et al*, 2008a). This analysis revealed that distal meristematic cell that in wild-type roots expresses the RCH2 marker line now expresses the *CYCB1;1:GUS* cell cycle reporter causing a shootward shift of the TZ in *expa1* as is the case of cytokinin signaling mutants (Fig EV1E and F; Dello Ioio *et al*, 2008a,b). Most importantly, measurements of length and area of root cells above the TZ in the *expa1* mutant revealed that these cells are considerably shorter and smaller than in wild-type roots (Fig 1H and I). Furthermore, the development of vascular xylem elements and root hairs was delayed in the *expa1* mutant, confirming a setback in cell differentiation (Fig 1E–G). These evidences suggest that the impairment in cell wall loosening and the resulting impairment in cell elongation, due to the lack of EXPA proteins activity, hamper cell differentiation.

To corroborate the notion that *EXPA* genes control cell differentiation, we analyzed their expression in the root. No signal was detected from Green Fluorescent Protein (GFP) translational fusions under the control of *EXPA* promoters although, for example, the *pEXPA1:EXPA1:GFP* was shown to be functional as it was capable of complementing the root meristem phenotype of the *expa1* mutant (Fig EV1G). In contrast, transcriptional fusions—*pEXPA1-GFP* and *pEXPA10-GUS*, *pEXPA14-GUS* and *pEXPA15-GUS*—revealed that *EXPA* genes are all expressed at the TZ, although in different tissues, but not in the meristem (Figs 1J and EV2B–D). Interestingly, *EXPA1* is the only one expressed in the epidermis TZ (and in the columella; Fig 1J), in agreement with the reported relevance of this tissue in coordinating cell expansion during root growth (Hacham *et al*, 2011; Fridman *et al*, 2014) and in being the source of instructive scaling and positional input in controlling organ size (Gruel *et al*, 2016). Altogether, these data indicate that *EXPA* genes are expressed at the TZ and that their activity in this root district is necessary to drive cell differentiation.

We next confirmed that, as previously reported (Bhargava *et al*, 2013), the *EXPA1*, *EXPA10*, *EXPA14,* and *EXPA15* genes are under the control of cytokinin (Figs 1K and EV2E). We have previously shown that the cytokinin-dependent ARR1 transcription factor is necessary and sufficient to control cytokinin-dependent cell differentiation initiation (Dello Ioio *et al*, 2008a; Di Mambro *et al*, 2017). Thus, we set to assess whether ARR1 has a direct control of the *EXPA1*, *EXPA10*, *EXPA14,* and *EXPA15* genes. Interestingly, ChIP-qPCR assay revealed that ARR1 directly binds the *EXPA1* promoter, while no enrichment could be detected for the *EXPA10*, *EXPA14,* and *EXPA15* promoters (Fig EV2A and F). Furthermore, no cytokinin induction of the *EXPA1* gene could be detected in the *arr1-4* mutant background (Fig 1K). ARR1 positively regulates *EXPA1* expression, as the transcript level of this gene was lower in the *arr1-4* mutant, while ARR1 overexpression resulted in activation of *EXPA1* (Fig 1K and L). ARR1 control on *EXPA1* expression is limited to the epidermis transition boundary, as no changes in *EXPA1* expression in the columella could be detected upon cytokinin treatments or in the *arr1-4* mutant background (Fig 1J). Thus, ARR1 directly and positively controls expression of the *EXPA1* gene, which in turn is necessary to control the position of the TZ, and root and root meristem size. In contrast, the *EXPA10*, *EXPA14,* and *EXPA15* genes act redundantly and their activities might be under the control of other cytokinin-dependent transcription factors.

To assess whether the EXPA1 protein is not only necessary but also sufficient to control cell differentiation, we ubiquitously expressed the *EXPA1* gene by means of the *UBQ10* promoter (*UBQ10-EXPA1*). As no root phenotype could be observed in *UBQ10-EXPA1* plants (Fig 2A and C), we hypothesized that in these plants the ectopic EXPA1 protein is not functional because it needs

Figure 1. *EXPA1* positively controls the initiation of meristematic cell differentiation.

A Confocal microscopy images of WT and *expa1* root tips. Changes in cell size at the cortex transition boundary (TB) in WT root are shown in the insert. The TB is a tissue-specific boundary where divisions cease and cells start to differentiate. The zone encompassing the TB of the different cell tissues represents the TZ. Blue and white arrowheads indicate the QC and the cortex TB, respectively.

B Root meristem cell number of WT and *expa1* mutant ($n = 60$. ***$P < 0.001$; Student's *t*-test).

C Seedling of WT and *expa1* mutant.

D Root length quantification of WT and *expa1* mutant ($n = 15$. ***$P < 0.001$; Student's *t*-test).

E Confocal images of WT and *expa1* root tip. White asterisk indicates the QC, yellow arrowheads indicate the first detectable root hair, and light blue arrowheads mark the first appearance of differentiated tracheids.

F, G Measurements of tracheids (F) and root hair (G) distance from the QC in WT and *expa1* root tips ($n = 10$. ***$P < 0.001$; Student's *t*-test).

H Measurement of cell length of newly differentiated cortex cells of WT and *expa1* roots ($n = 15$).

I Measurement of cell area of newly differentiated cortex cells of WT and *expa1* roots ($n = 15$).

J Confocal microscopy images of roots expressing the *pEXPA1::ER-GFP* construct in WT ($n = 20$), in *arr1-4* ($n = 15$) mutant backgrounds and of *pEXPA1::ER-GFP* root upon cytokinin treatments ($n = 15$), respectively. *pEXPA1::ER-GFP*-specific expression at the epidermis TB is shown in the insert.

K qRT–PCR analysis of *EXPA1* mRNA levels in the root tip of WT, *arr1-4*, and cytokinin-treated WT and *arr1-4* roots (**$P < 0.01$, ***$P < 0.001$, n.s. corresponds to not significant; Student's *t*-test; three technical replicates performed on two independent RNA batches).

L qRT–PCR analysis of *EXPA1* mRNA levels in the root tip of *35S::ARR1ΔDDK:GR* plants upon dexamethasone (Dex) treatments. The value for the control mock-treated WT was set to 1, and the relative values are reported (**$P < 0.01$; Student's *t*-test; three technical replicates performed on two independent RNA batches).

Data information: In (A-L), experiments were performed on seedlings at 5 dpg. Error bars indicate SD.

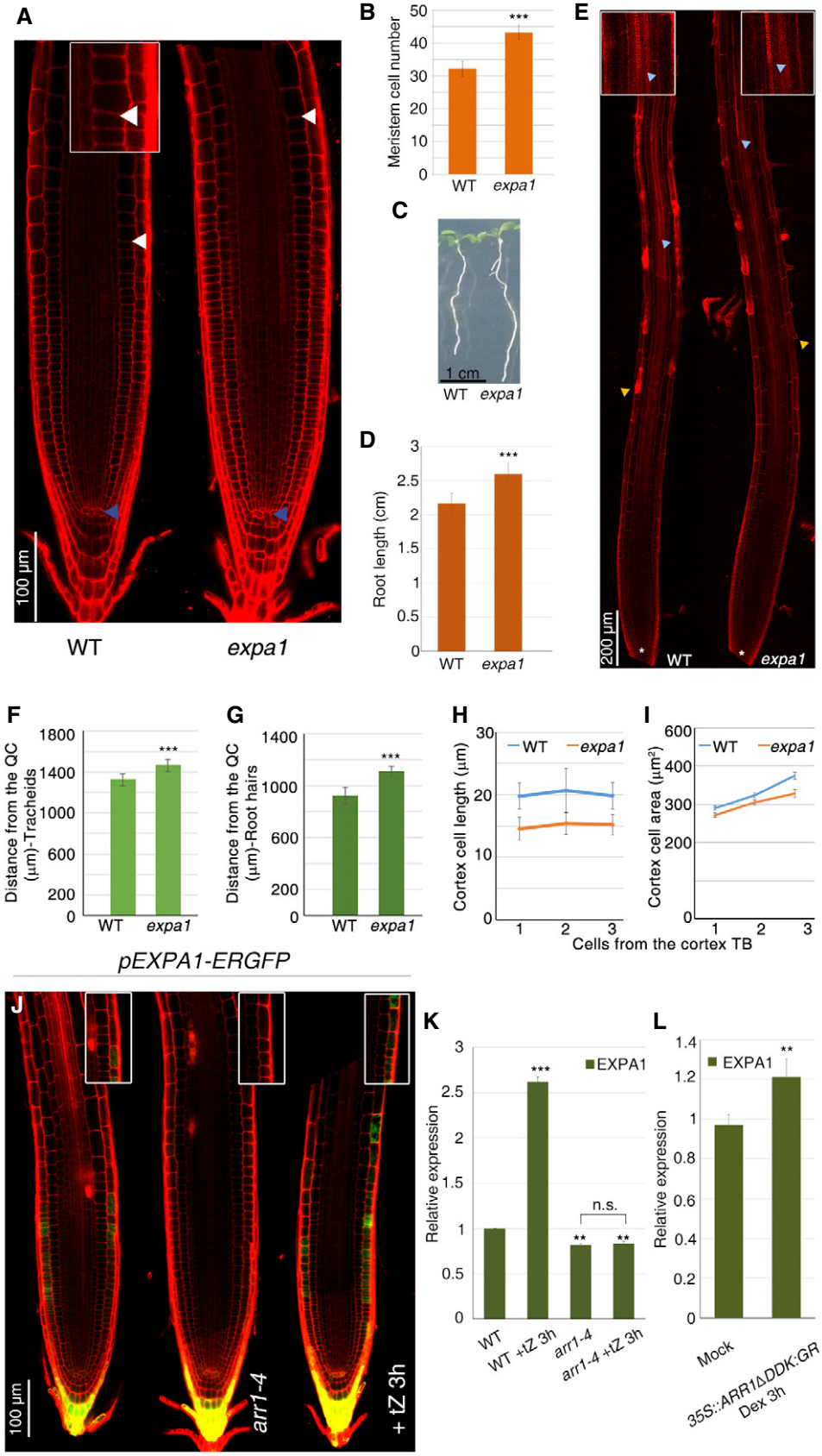

Figure 1.

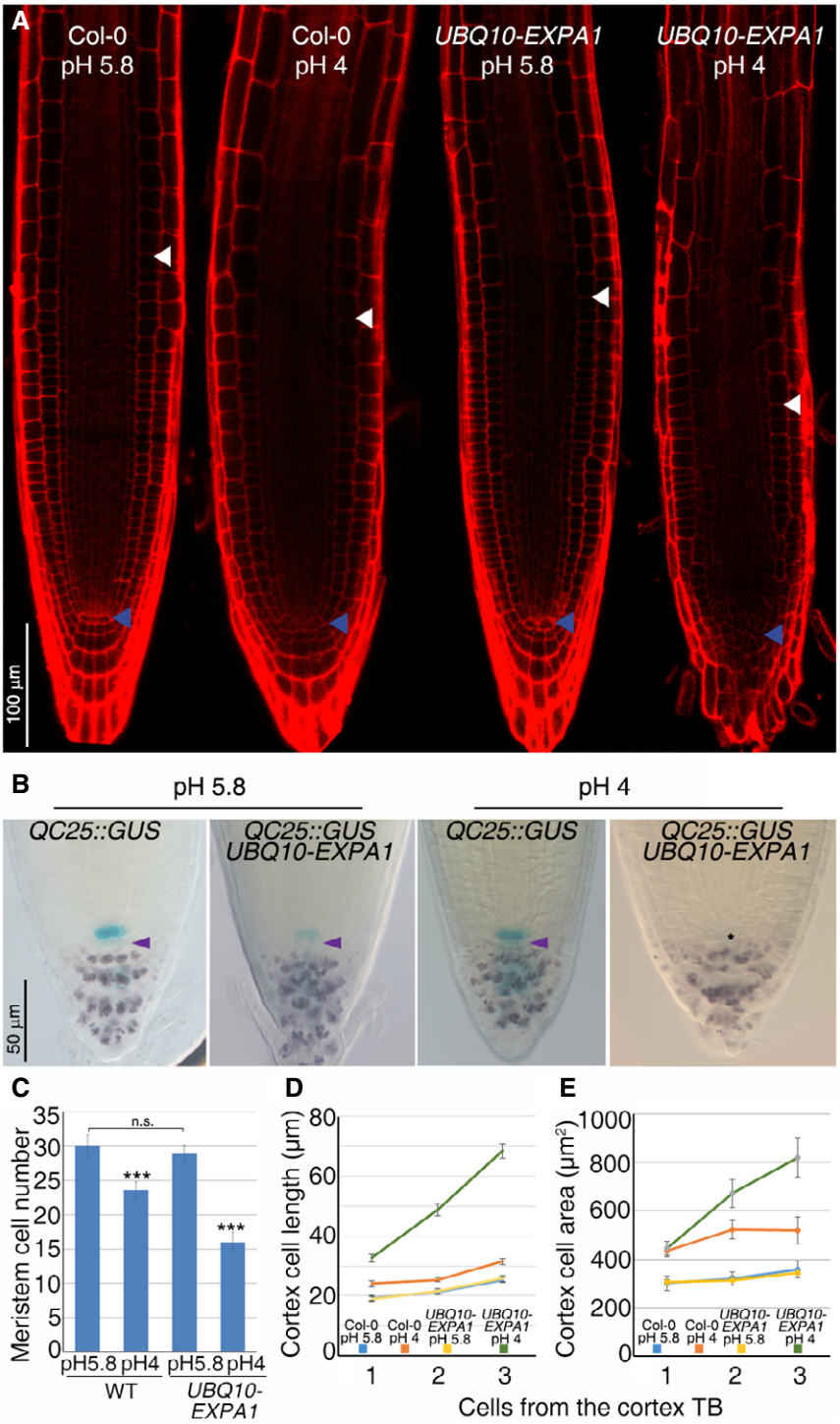

Figure 2. Activated EXPA1 protein induces cell differentiation revealing its function *in vivo*.

A Confocal microscopy images of WT and *UBQ10-EXPA1* root tips grown on standard (5.8) or acidic (4.0) pH. Blue and white arrowheads indicate the QC and the cortex TB, respectively.

B Stem cell niche expressing the QC-specific marker (QC25) of WT and *UBQ10-EXPA1* root tips grown on standard (5.8) or acidic (4.0) pH. Lugol staining highlights differentiated columella cells. Violet arrowheads indicate columella stem cells. Asterisk indicates the presumptive position of QC cells in *UBQ10-EXPA1* root grown on pH 4.

C Meristem cell number of WT and *UBQ10-EXPA1* grown on standard and acidic pH (n = 30. ***P < 0.001, n.s. corresponds to not significant; Student's t-test).

D Measurement of cell length of newly differentiated cortex cells of WT and *UBQ10-EXPA1* root tips grown on standard or acidic pH (n = 15; three replicates).

E Measurement of cell area of newly differentiated cortex cells of WT and *UBQ10-EXPA1* root tips grown on standard or acidic pH (n = 15; three replicates).

Data information: In (A–E), experiments were performed on seedlings at 5 dpg. In (C–E), error bars indicate SD.

low apoplastic pH to be activated (Sampedro & Cosgrove, 2005). To verify this hypothesis, we germinated *UBQ10-EXPA1* plants on a medium adjusted to pH 4. These are the optimal acidic conditions for EXPA proteins activation (Sampedro & Cosgrove, 2005) and have little effects on WT root meristematic activities (Gujas *et al*, 2012; Fig 2A and C). Indeed, in these conditions, the root of *UBQ10-EXPA1* plants stopped growing and the root meristem was dramatically reduced compared to wild-type roots, due to premature cell differentiation (Figs 2A and C, and EV2G and H). In the root meristem of these plants, the stem cell niche was very disorganized. Analysis of QC-specific markers revealed loss of QC and stem cell function as cells immediately below the QC, at the position of columella stem cell, acquired differentiation markers such as amyloplasts (Fig 2B). Furthermore, the length and area of newly

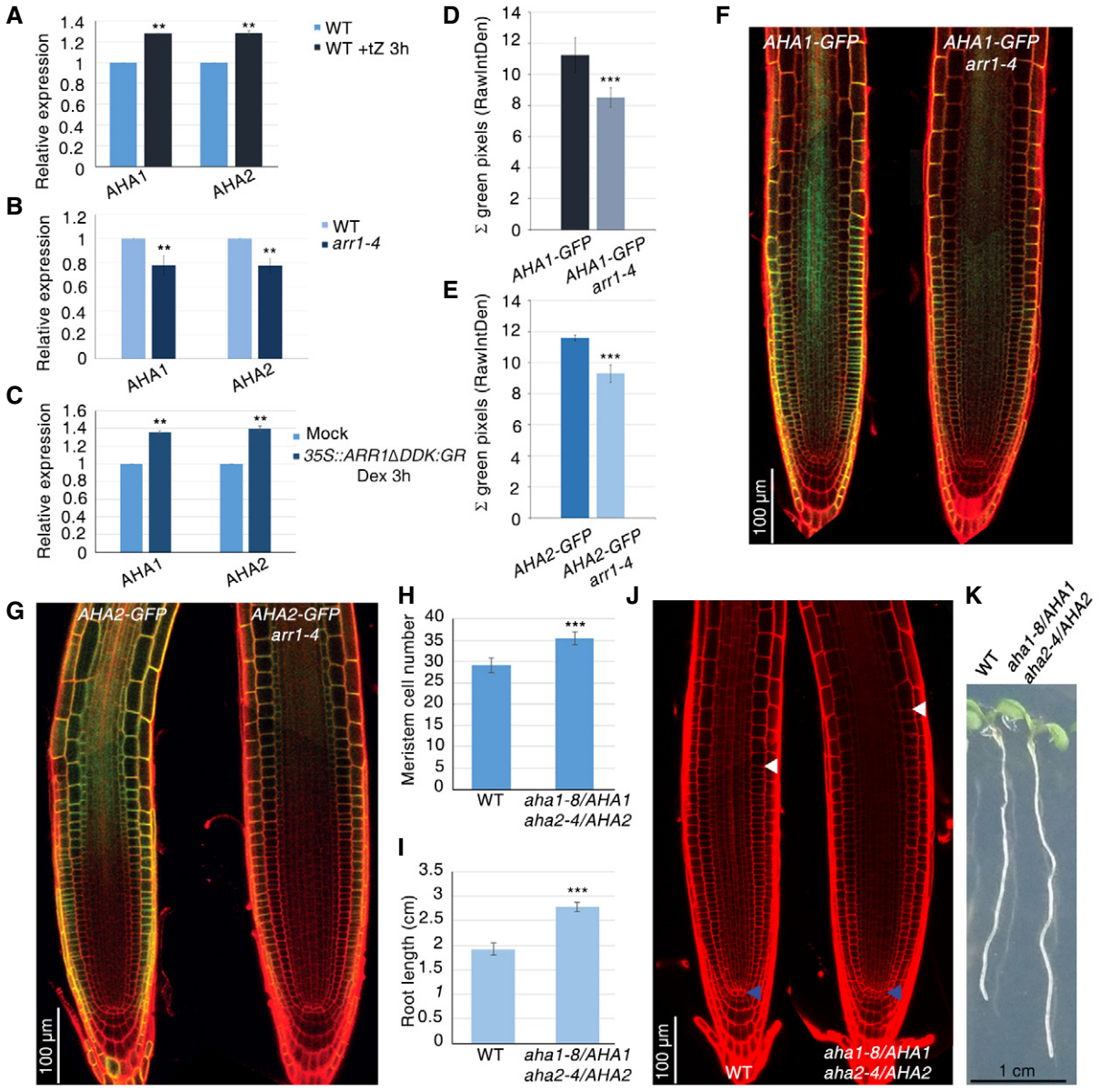

Figure 3. AHA1 and AHA2 control meristematic cell differentiation initiation.

A–C qRT–PCR analysis of *AHA1* and *AHA2* mRNA levels in WT root tip upon cytokinin treatment (A) in the root tip of *arr1-4* mutant (B) and in the root tip of *35S::ARR1ΔDDK:GR* plants upon Dex induction (C) (**$P < 0.001$; Student's *t*-test; three technical replicates performed on two independent RNA batches).

D, E Relative fluorescence quantification of roots depicted in (F) and (G), respectively ($n = 10$. ***$P < 0.001$; Student's *t*-test).

F, G Confocal microscopy images of WT ($n = 20$) and *arr1-4* ($n = 20$) roots expressing the *AHA1-GFP* construct (F) and the *AHA2-GFP* construct (G).

H, I Root meristem cell number ($n = 60$) (H) and root length ($n = 20$) (I) of WT and *aha1-8/AHA1;aha2-4/AHA2* mutant (***$P < 0.001$; Student's *t*-test).

J Confocal microscopy images of WT and *aha1-8/AHA1;aha2-4/AHA2* roots meristem. Blue and white arrowheads indicate the QC and the cortex TB, respectively.

K Seedlings of WT and the *aha1-8/AHA1;aha2-4/AHA2* mutant.

Data information: In (A–K), experiments were performed on seedlings at 5 dpg. Error bars indicate SD.

differentiated cells were increased (Fig 2D and E). The same results were obtained overexpressing EXPA10, EXPA14, and EXPA15 in plants grown in acidic medium (Fig EV2I). These data confirm that low apoplastic pH activates the EXPA proteins and that probably by loosening the cell wall these proteins cause a change in the shape of the cell thus inducing stem cell and meristematic cell differentiation.

In plants, acidification of the apoplast is guaranteed by the plasma membrane H^+-ATPases (HA), electrogenic enzymes that transport protons (H^+) out of the cell, thus regulating cellular pH homeostasis (Haruta *et al*, 2015). In *Arabidopsis*, *AHA1* and *AHA2* (*Arabidopsis HA* 1 and 2) are active in the primary root (Baxter *et al*, 2003). We thus wondered whether to induce cell differentiation via the *EXPA* genes cytokinin also controls the expression of the *AHA1* and *AHA2* genes. Indeed, exposure of WT roots to exogenous cytokinin resulted in induction of *AHA1* and *AHA2* expression as shown by RT–PCR (Fig 3A). In accordance, ChIP-qPCR assay revealed that ARR1 binds intronic regions of both *AHA1* and *AHA2* (Fig EV3A). Furthermore, *AHA1* and *AHA2* are down-regulated in the *arr1-4* mutant background (Fig 3B and D–G), while overexpression of ARR1 results in *AHA1* and *AHA2* induction (Fig 3C). Thus, cytokinin, via ARR1, directly controls expression of the *EXPA1* gene and of the *AHA1* and *AHA2* genes.

In order to establish whether the AHA1 and AHA2 proton pumps mediate apoplast acidification in the same domain of EXPA proteins activity, we set to analyze the expression pattern of the *AHA1* and *AHA2* genes in the root by generating GFP translational fusions (*AHA1-GFP* and *AHA2-GFP* plants). Analysis of these plants revealed that both genes are expressed at the TZ, with AHA1 showing a broad expression domain across the meristematic region, while AHA2 is more specifically localized at the TZ (Fig 3F and G). This expression is in accordance with the pH drop observed at the TZ in the *Arabidopsis* root (Staal *et al*, 2011).

We reasoned that, if (by mediating apoplastic acidification) the AHA1 and AHA2 proteins activate expansins, mutation in these genes would result in altered cell differentiation initiation and thus TZ position and root and root meristem size. However, analysis of the *aha1-8* and *aha2-4* loss-of-function mutants revealed no root phenotype (Fig EV3B). It was previously reported that the double homozygous *aha1,aha2* mutant causes embryo lethality (Haruta *et al*, 2010). We thus analyzed the double heterozygous mutant, *aha1-8/AHA1;aha2-4/AHA2,* hypothesizing that these genes would act together in a dose-dependent fashion. Indeed, as predicted, the *aha1-8/AHA1;aha2-4/AHA2* double heterozygous mutants displayed larger meristems and longer roots compared to WT (Fig 3H–K). To verify whether this change in root meristem size is accompanied by changes in root apoplastic pH, we measured the capability of the *aha1-8/AHA1;aha2-4/AHA2* mutant roots to acidify the medium. To this end, we transferred *aha1-8/AHA1;aha2-4/AHA2* mutant seedlings onto medium containing a pH indicator. As expected, in this mutant, the acidification capability of the roots is decreased compared to the wild type and to the single *aha1-8* and *aha2-4* mutants, implying that H^+ proton export in the medium (and in the apoplast) is decreased (Fig EV3C). This confirms that the AHA1 and AHA2 proton pumps are necessary to mediate apoplastic pH acidification and suggests that they are involved in controlling root meristem cell differentiation. To further establish the role of the *AHA1* and *AHA2* in root meristem size determination, we generated plants ubiquitously expressing these genes (*UBQ10-AHA1* and *UBQ10-AHA2* plants). These plants failed to complete their development and died (data not shown). We thus created an inducible version of the *pUBQ10-AHA2* construct (*pUBQ10::AHA2:GR*). Interestingly, upon 20 h of dexamethasone (Dex) treatment, *pUBQ10::*

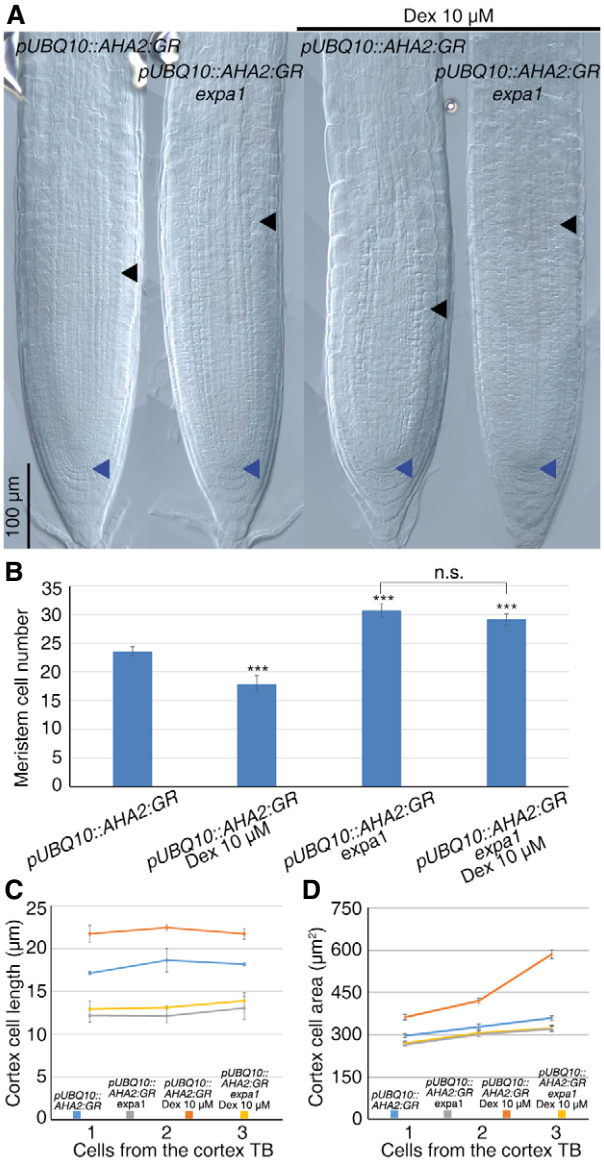

Figure 4. AHA1- and AHA2-dependent apoplast acidification activates EXPA1 and induces cell differentiation.

A DIC microscopy images of WT and *expa1* roots expressing the p*UBQ10::AHA2:GR* construct treated and untreated with Dex. Blue and black arrowheads indicate the QC and the cortex TB, respectively.

B Measurement of meristem cell number of roots depicted in a (n = 30. For statistical analysis, untreated *pUBQ10::AHA2:GR* was set as reference. ***$P < 0.001$, n.s. corresponds to not significant; Student's t-test).

C Measurement of cell length of newly differentiated cortex cells of root depicted in (A) (n = 15).

D Measurement of cell area of newly differentiated cortex cells of root depicted in (A) (n = 15).

Data information: In (A–D), experiments were performed on seedlings at 5 dpg. Error bars indicate SD.

AHA2:GR plants showed a drastic reduction in root meristem size compared to WT (Fig 4A and B). Moreover, the length and area of newly differentiated cells were increased as in the case of *UBQ10-EXPA1* plants grown on acidic medium (Fig 4C and D). Thus, apoplastic acidification of the root mediated by the AHA1 and AHA2 proton pumps is necessary to control initiation of cell differentiation, to position the TZ and thus define root and root meristem size.

We next asked whether the apoplastic acidification caused by the AHAs drives cell differentiation by activating EXPA activity. To this aim, we crossed plants harboring the *pUBQ10::AHA2:GR* construct with the *expa1* mutant. Interestingly, while a 20-h Dex treatment of *pUBQ10::AHA2:GR* plants resulted in a reduction in meristem size, no changes in meristem and cell size were observed in *pUBQ10::AHA2:GR;expa1* plants (Fig 4A and C). Thus, acidification of the apoplast mediated by AHA2 activates the EXPA1 protein that, in turn, likely by loosening the cell wall, allows cell expansion and promotes cell differentiation.

In conclusion, we show here that cytokinin directly controls, via ARR1, the activity of the *EXPA1* gene and, at the same time, of the *AHA1* and *AHA2* genes. This creates the pH conditions at the TZ for the EXPA1 protein to induce cell wall loosening and consequently cell elongation, thus driving cell differentiation; this controls the position of the TZ and consequently root and root meristem size. We have previously shown that cytokinin determines the position of the TZ by positioning an auxin minimum in the topmost meristematic cell and that cytokinin treatment moves this auxin minimum into the meristem before cell elongation can be observed (Di Mambro *et al*, 2017). It is thus tempting to propose a model where in the *Arabidopsis* root cytokinin first establishes the position of the auxin minimum, which provides to the topmost meristematic cell of each tissue the competence to differentiate; in these competent cells, the activities of both EXPA and AHA proteins result in a sudden change in volume (elongation) that is the functional trigger of differentiation (Fig EV3D). Accordingly, if the pH conditions are not optimal, and/or the cell wall loosening capacities are impaired, cell differentiation is delayed.

Our results provide clear evidence that cell wall remodeling due to acidification and expansin-dependent loosening brings about a change in cell shape (dimensions) that has an important role in controlling the cell differentiation program.

Materials and Methods

Data reporting

No statistical methods were used to predetermine sample size. The experiments were not randomized, and the investigators were not blinded to allocation during experiments and outcome assessment.

Plant material and growth conditions

All mutants are in the *Arabidopsis thaliana* Col-0 ecotype. *arr1-4* allele was previously described in Dello Ioio *et al*, 2007, and *aha1-8* and *aha2-4* alleles were previously described in Haruta *et al* (2010). *expa1-1*, *expa10-1*, *expa14-1*, and *expa15-1* alleles were obtained from the Nottingham *Arabidopsis* Stock Centre collection (SALK_010506, SALK_053326, SALK_089449, and SALK_107975, respectively). Homozygous mutants from the Salk T-DNA were identified by PCR as described (http://signal.salk.edu/).

For growth conditions, *Arabidopsis* seeds were surface sterilized, and seedlings were grown on one-half-strength Murashige and Skoog (MS) medium containing 0.8% agar at 22°C in long-day conditions (16-h-light/8-h-dark cycle) as previously described in Perilli and Sabatini (2010).

In the experiments involving pH variation, the pH of the medium was adjusted using HCl before adding agar and autoclaving (Gujas *et al*, 2012).

Root length and meristem size analysis

Root meristem size for each plant was measured based on the number of cortex cells in a file extending from the quiescent center to the first elongated cortex cell excluded, as described previously (Perilli and Sabatini, 2010). The cortex is the most suitable tissue to count meristematic cells, as its single cell type composition shows a conserved number of cells among different roots. The boundary between dividing and differentiating cells for each tissue is called transition boundary (TB), while the region including the different transition boundaries is called transition zone (TZ; Di Mambro *et al*, 2017). Cell-o-Tape (French *et al*, 2012), a Fiji (http://fiji.sc/Fiji) macro, was used to confirm the position of the last cortical cell at the TB. Images were obtained using a confocal laser scanning microscope (Zeiss LSM 780). Student's *t*-test was used to determine statistical significance of these data (http://graphpad.com/quickcalcs/ttest2.cfm).

Lugol staining

Starch granules in the root tips were stained with Lugol's solution (Carlo Erba Reagenti) for few seconds and then immediately observed and photographed at microscopy as previously described (Sabatini *et al*, 2003).

RNA isolation and RT–qPCR

Total RNA was extracted from 5 days post-germination roots using the NucleoSpin RNA Plus (Macherey-Nagel), and the first-strand cDNA was synthesized using the Superscript® III First-Strand Synthesis System (Invitrogen). Quantitative RT–PCR analysis was conducted using gene-specific oligonucleotides primers (Appendix Table S1). PCR amplification was carried out in the presence of the double-strand DNA-specific dye SsoAdvanced Universal SYBR Green Supermix (Bio-Rad). Amplification was monitored in real time with the 7500 Fast Real-Time PCR System (Applied Biosystems) according to the manufacturer's instructions. Experiments were performed in triplicates from two independent RNA extractions. Data were analyzed using the $\Delta\Delta C_t$ (cycle threshold) method and normalized with the expression of the reference gene ACTIN2 (ACT2). Student's *t*-test was used to determine statistical significance of these data (http://graphpad.com/quickcalcs/ttest2.cfm).

ChIP-qPCR

The enrichment of the *EXPA1* target promoter regions DNA and the *AHA1* and *AHA2* intronic regions DNA in the immunoprecipitated *pARR1:ARR1:GFP* DNA (Di Mambro *et al*, 2017) was confirmed using

RT–qPCR. A qPCR efficiency of twofold amplifications per cycle was assumed, and a sequence from *ACT2* was used to normalize the results between samples. PCR amplification was carried out in the presence of the double-strand DNA-specific dye SsoAdvanced Universal SYBR Green Supermix (Bio-Rad). Amplification was monitored in real time with the 7500 Fast Real-Time PCR System (Applied Biosystems). Experiments were performed in duplicate from two independent immunoprecipitated chromatin batches. This analysis was done using sets of adjacent specific amplified regions (Appendix Table S1). Student's *t*-test was used to determine statistical significance of these data (http://graphpad.com/quickcalcs/ttest2.cfm).

Transgenic lines generation

Genomic DNA from *Arabidopsis* ecotype Columbia (Col-0) was used as the template for amplification. *pEXPA1:ER-GFP* transcriptional fusion was generated utilizing the Gateway system (Invitrogen). The 1,886 base pairs (bp) region upstream of the *EXPA1* ATG was amplified using the pEXPA1 primers (Appendix Table S1), and the PCR product was then cloned in pENTR5'-TOPO TA vector. Subsequently, pENTR5′-TOPO TA-pEXPA1 and pDONOR221-ER-GFP were recombined with pDONR P2R_P3-NOS into a pBm43GW destination vector via LR reaction (Invitrogen). *pEXPA10-GUS*, *pEXPA14-GUS,* and *pEXPA15-GUS* transcriptional fusion were generated utilizing the Gateway system (Invitrogen). The 2,040 bp region upstream of the *EXPA10* ATG, the 2,001 bp region upstream of the EXPA14 ATG, and the 2,003 bp region upstream of the EXPA15 ATG were amplified using the pEXPA10, pEXPA14, and pEXPA15 primers (Appendix Table S1), respectively. pENTR5′-TOPO TA-pEXPA10, pENTR5′-TOPO TA-pEXPA14, pENTR5′-TOPO TA-pEXPA15, and a pDONOR221-GUS vector were recombined with pDONR P2R_P3-NOS into a pBm43GW destination vector via LR reaction (Invitrogen). *UBQ10-EXPA1, UBQ10-EXPA10*, *UBQ10-EXPA14,* and *UBQ10-EXPA15* constructs were obtained as follows. The *EXPA1, EXPA10*, *EXPA14,* and *EXPA15* sequences were amplified using the gEXPA1, gEXPA10, gEXPA14, and gEXPA15 primers (Appendix Table S1) and cloned in pDONR221 Gateway vector by BP recombination (Invitrogen). Subsequently, pDONR221-EXPA1, pDONR221-EXPA10, pDONR221-EXPA14, and pDONR221-EXPA15, respectively, were recombined with a pDONRP4_P1R-pUBQ10 vector and pDONRP2R_P3-NOS into a pBm43GW destination vector via LR reaction (Invitrogen). To generate *AHA1-GFP* and *AHA2-GFP* constructs, the 1,930 bp region upstream of the *AHA1* ATG and the 1,819 bp region upstream of the AHA2 ATG were amplified using the pAHA1 and pAHA2 primers (Appendix Table S1), respectively, and the PCR product was then cloned in pENTR5′-TOPO TA vector. The *AHA1* and *AHA2* sequences were amplified using the gAHA1 and gAHA2 primers (Appendix Table S1) and cloned in pDONR221 Gateway vector by BP recombination (Invitrogen). Subsequently, pDONRP4_P1R-pAHA1 and pDONR221-AHA1 and pDONRP4_P1R-pAHA2 and pDONR221-AHA2 were recombined with pDONR P2R_P3-C-term GFP into a pBm43GW destination vector via LR reaction (Invitrogen). *pUBQ10::AHA2:GR* construct was obtained as follows. The pDONRP4_P1R-pUBQ10 vector and pDONR221-AHA2 vector were recombined with pDONRP2R_P3-GR into a pB7m34GW destination vector via LR reaction (Invitrogen). Plasmids were transformed into Col-0 plants by floral dipping (Clough & Bent, 1998). For each T3 generation, four independent homozygous lines of transgenic plants were analyzed. *AHA1-GFP* and *AHA2-GFP* translational fusions rescue the *AHA1/aha1;AHA2/aha2* mutant phenotype.

GUS histochemical assay

GUS histochemical assay was performed as described in Perilli and Sabatini (2010). Five-day-old seedlings were incubated for 16 h at 37°C in the dark and imaged using the Axio Imager.A2 (Zeiss) microscope.

Fluorescence quantification

The fluorescence intensity of plants carrying *AHA1-GFP* and *AHA2-GFP* was quantified by the plugin MeasureRGB of the software ImageJ on confocal laser scanning microscope images taking as ROI the expression domain of AHA1 and AHA2, respectively. Student's *t*-test was used to determine statistical significance of these data (http://graphpad.com/quickcalcs/ttest2.cfm).

Hormonal treatments

Five-day-old seedlings were transferred to solid one-half MS medium containing mock conditions or a suitable concentration of hormone. For cytokinin treatment, we used trans-zeatin (tZ, Duchefa) at a final concentration of 5 μM. For dexamethasone (Dex, Sigma) treatment, a final concentration of 10 μM was used. For DEX treatments, mock represents the MS media supplemented with ethanol. For tZ treatments, mock signifies MS media supplemented with dimethyl sulfoxide.

Rhizosphere acidification assays

To visualize rhizosphere acidification, 5-day-old seedlings were transferred to one-half-strength MS-agar plates supplemented with 0.003% bromocresol purple (Sigma-Aldrich) (sensitivity range pH 5.2–6.8). The plates were incubated in the same culture chamber and scanned after 16 h. Comparisons were made with a color bar generated by documenting the color change of bromocresol purple in the same medium at specific pH values.

Expanded View for this article is available online.

Acknowledgements

We thank Elena Salvi, Emanuela Pierdonati, and Laura Polverari for critical reading of the manuscript. We thank GrassRoots Biotechnology, Inc. for providing the pDONORP4P1-pUBQ10 vector, pub. no. WO/2012/006426. We thank Philip N. Benfey and Renze Heidstra for providing materials. This work was supported by The European Research Council (to S.S. and E.P.), FIRB (Futuro in Ricerca 2013) (to R.D.I. and E.P.), and by grant from Sapienza University (to P.C.).

Author contributions

EP planned and performed experiments. RDM and RDI performed experiments. EP, SS, and PC discussed and interpreted all results and wrote the manuscript. SS conceived the research.

Conflict of interest

The authors declare that they have no conflict of interest.

References

Baxter I, Tchieu J, Sussman MR, Boutry M, Palmgren MG, Gribskov M, Harper JF, Axelsen KB (2003) Genomic comparison of P-type ATPase ion pumps in *Arabidopsis* and rice. *Plant Physiol* 132: 618 – 628

Benfey PN, Scheres B (2000) Root development. *Curr Biol* 10: R813 – R815

Bhargava A, Clabaugh I, To JP, Maxwell BB, Chiang Y-H, Schaller GE, Loraine A, Kieber JJ (2013) Identification of cytokinin-responsive genes using microarray meta-analysis and RNA-Seq in *Arabidopsis*. *Plant Physiol* 162: 272 – 294

Cho H-T, Cosgrove DJ (2000) Altered expression of expansin modulates leaf growth and pedicel abscission in *Arabidopsis thaliana*. *Proc Natl Acad Sci* 97: 9783 – 9788

Clough SJ, Bent A (1998) Floral dip: a simplified method for Agrobacterium-mediated transformation of *Arabidopsis thaliana*. *Plant J* 16: 735 – 743

Cosgrove DJ (2005) Growth of the plant cell wall. *Nat Rev Mol Cell Biol* 6: 850 – 861

Dello Ioio R, Linhares FS, Sabatini S (2008a) Emerging role of cytokinin as a regulator of cellular differentiation. *Curr Opin Plant Biol* 11: 23 – 27

Dello Ioio R, Linhares FS, Scacchi E, Casamitjana-Martinez E, Heidstra R, Costantino P, Sabatini S (2007) Cytokinins determine Arabidopsis root-meristem size by controlling cell differentiation. *Curr Biol* 17: 678 – 682

Dello Ioio R, Nakamura K, Moubayidin L, Perilli S, Taniguchi M, Morita MT, Aoyama T, Costantino P, Sabatini S (2008b) A genetic framework for the control of cell division and differentiation in the root meristem. *Science* 322: 1380 – 1384

Di Mambro R, De Ruvo M, Pacifici E, Salvi E, Sozzani R, Benfey PN, Busch W, Novak O, Ljung K, Di Paola L, Marée AFM, Costantino P, Grieneisen VA, Sabatini S (2017) Auxin minimum triggers the developmental switch from cell division to cell differentiation in the *Arabidopsis* root. *Proc Natl Acad Sci* 114: E7641 – E7649

French AP, Wilson MH, Kenobi K, Dietrich D, Voß U, Ubeda-Tomás S, Pridmore TP, Wells DM (2012) Identifying biological landmarks using a novel cell measuring image analysis tool: cell-o-Tape. *Plant Methods* 8: 7

Fridman Y, Elkouby L, Holland N, Vragović K, Elbaum R, Savaldi-Goldstein S (2014) Root growth is modulated by differential hormonal sensitivity in neighboring cells. *Genes Dev* 28: 912 – 920

Gruel J, Landrein B, Tarr P, Schuster C, Refahi Y, Sampathkumar A, Hamant O, Meyerowitz EM, Jönsson H (2016) An epidermis-driven mechanism positions and scales stem cell niches in plants. *Sci Adv* 2: e1500989

Gujas B, Alonso-Blanco C, Hardtke CS (2012) Natural *Arabidopsis* brx loss-of-function alleles confer root adaptation to acidic soil. *Curr Biol* 22: 1962 – 1968

Hacham Y, Holland N, Butterfield C, Ubeda-Tomas S, Bennett MJ, Chory J, Savaldi-Goldstein S (2011) Brassinosteroid perception in the epidermis controls root meristem size. *Development* 138: 839 – 848

Haruta M, Burch HL, Nelson RB, Barrett-Wilt G, Kline KG, Mohsin SB, Young JC, Otegui MS, Sussman MR (2010) Molecular characterization of mutant *Arabidopsis* plants with reduced plasma membrane proton pump activity. *J Biol Chem* 285: 17918 – 17929

Haruta M, Gray WM, Sussman MR (2015) Regulation of the plasma membrane proton pump (H + -ATPase) by phosphorylation. *Curr Opin Plant Biol* 28: 68 – 75

Marshall WF, Young KD, Swaffer M, Wood E, Nurse P, Kimura A, Frankel J, Wallingford J, Walbot V, Qu X, Roeder AHK (2012) What determines cell size? *BMC Biol* 10: 101

Pacifici E, Polverari L, Sabatini S (2015) Plant hormone cross-talk: the pivot of root growth. *J Exp Bot* 66: 1113 – 1121

Perilli S, Sabatini S (2010) Analysis of root meristem size development. *Methods Mol Biol* 655: 177 – 187

Sabatini S, Heidstra R, Wildwater M, Scheres B (2003) SCARECROW is involved in positioning the stem cell niche in the *Arabidopsis* root meristem. *Genes Dev* 17: 354 – 358

Sampedro J, Cosgrove DJ (2005) The expansin superfamily. *Genome Biol* 6: 242

Staal M, De Cnodder T, Simon D, Vandenbussche F, Van der Straeten D, Verbelen J-P, Elzenga T, Vissenberg K (2011) Apoplastic alkalinization is instrumental for the inhibition of cell elongation in the *Arabidopsis* root by the ethylene precursor 1-aminocyclopropane-1-carboxylic acid. *Plant Physiol* 155: 2049 – 2055